Published in Nano Energy, doi: 10.1016/j.nanoen.2021.106045 (2021).

On the Evaluation of Output Voltages for Quantifying the Performance of Pyroelectric Energy Harvesters

Qinlan Li, [a,b] Shuang Li, [a,b] Dario Pisignano,[c] Luana Persano, [d] Ya Yang, [e] Yewang Su [a,b,f*]

[a] *State Key Laboratory of Nonlinear Mechanics, Institute of Mechanics, Chinese Academy of Sciences, Beijing 100190, China*

[b] *School of Engineering Science, University of Chinese Academy of Sciences, Beijing 100049, China*

[c] *Dipartimento di Fisica, Università di Pisa, Largo B. Pontecorvo 3, I-56127 Pisa, Italy*

[d] *NEST, Istituto Nanoscienze-CNR, Piazza S. Silvestro 12, I-56127 Pisa, Italy*

[e] *CAS Center for Excellence in Nanoscience, Beijing Key Laboratory of Micro-nano Energy and Sensor, Beijing Institute of Nanoenergy and Nanosystems, Chinese Academy of Sciences, Beijing, 100083, China*

[f] *State Key Laboratory of Structural Analysis for Industrial Equipment, Department of Engineering Mechanics, Dalian University of Technology, Dalian 116024, China*

[*] To whom all correspondence should be addressed: yewangsu@imech.ac.cn

Published in Nano Energy, doi: 10.1016/j.nanoen.2021.106045 (2021).

Abstract

Pyroelectric energy harvesters (PyEHs) have been extensively developed for the energy supply to wireless, low-power advanced devices. Plenty of experiments show that the voltage–time curves for evaluating pyroelectric devices are alternatively positive and negative, while the fundamental pyroelectric theory gives a positive voltage without the negative portion. Here, this key confliction is addressed by both theoretical and experimental investigation. The voltage-time curves are recorded by three voltmeters with inner resistances of 10 MΩ, 150 GΩ, and 200 TΩ, respectively. Measured output voltages are found to be influenced greatly by the voltmeter's resistance and capacitance, with peak voltages differing by a factor that exceed 2,200. The performance of the PyEH should be characterized by the intrinsic voltage rather than the open-circuit voltage. As a significant conclusion, the resistance and capacitance of voltmeters used should be reported in the literature, thus providing a rational for comparing the performance of different devices.

1. Introduction

Since the early 2000s, wireless, low-power advanced devices including wearable electronics,[1] implantable electronics,[2] micro-sensors for structural health monitoring,[3] etc., have attracted extensive interest due to their wide range of potential applications.[4] The systems consisting of advanced energy harvesters and new energy storage technologies,[5-7] such as supercapacitors,[8] are investigated for the energy supply enabling continued operation of these devices, whereas conventional batteries are generally too bulky and environmentally unfriendly to power miniaturized and widely utilized components.[4, 7] Pyroelectric energy harvester (PyEH),[9-13] which is capable of converting the temperature fluctuation into electrical energy, is one of the most popular classes of devices in this framework. The basic mechanism of the PyEH is illustrated in **Fig. 1**a. The electrical potential difference is yielded between the top and bottom surfaces, when a pyroelectric film with polarization direction along the thickness direction is subjected to heating or cooling.[9] For the purpose of the energy supply, various PyEHs based on different pyroelectric materials are developed.[14-28] In all cases, the output voltage is a critical parameter to determine the performance of the PyEH. For example, Yang et al.[29] fabricated a pyroelectric nanogenerator using lead-free $KNbO_3$ nanowires that can yield a peak open-circuit voltage of about 10 mV, while a temperature change of $\Delta T_{max} \approx 40$ °C is applied. Wang et al.[30] presented a thermal nanophotonic-pyroelectric scheme consisting of the pyroelectric layer and metamaterial layers, which is able to transfer the solar energy to heat energy and electric energy. The maximum open-circuit voltage 5.4 V is obtained for the temperature fluctuation $\Delta T_{max} = 15.9$ °C. The influence of the electrode structure of the pyroelectric film on the thermal-electric conversion is studied by Zabek et al.[31] The temperature variation of $\Delta T_{max} = 2.8$ °C yields a peak open-circuit voltage of 59 V.

Accurate measurements of the open-circuit voltage are crucial to determine the performance of the PyEHs. Experiments in the literature show that, even though the applied temperature fluctuation ΔT is always positive (Fig. 1b), the voltage–time curves of pyroelectric devices encompass both positive and negative characteristics (Fig. 1c).[18-34] However, the pyroelectric theory of the open circuit, which is usually used to predict the peak of the voltage–time curve in the literature,[21-26, 30, 35] gives a different output voltage, namely (Fig. 1d):

$$V = \frac{(-p_3)d}{k_{33}}\Delta T\,, \tag{1}$$

where p_3, k_{33}, and d are the pyroelectric coefficient, the permittivity and the thickness of the pyroelectric film, respectively. By the pyroelectric theory of the open circuit, the open-circuit voltage should be proportional to the temperature fluctuation. The voltage is zero in the regime without heating, reaches the peak while the temperature is maximum and restores to zero after cooling. The output voltage is always positive during the heating-cooling cycles (Fig. 1d), which significantly conflicts with the experimental findings (Fig. 1c). In this study, we both investigate the theory model and carry out experimental measurements to address this critically important problem.

2. Results

In order to study the measurement of the output voltage, a square capacitor-type PyEH (area: A = 2 cm × 2 cm) consisting of a Poly(vinylidene fluoride) (PVDF) film between the top and bottom silver electrodes (15 μm/80 μm/15 μm), is prepared as shown in **Fig. S1**a. The PVDF film is transversely isotropic with a polarization direction normal to the surface. The pyroelectric coefficient, permittivity, and volume resistivity are p_3 = -2.5×10^{-5} C m^{-2} K^{-1}, k_{33} = 7×10^{-11} F m^{-1}, and ρ = 8×10^{12}

Ω m, respectively. The copper clad laminate is connected to the silver electrodes by conductive silver glues for the voltage measurement. For the performance characterization of the PyEH, a temperature controller integrating two Peltier modules, an NTC thermistor, two thermal pads, two heatsinks and a temperature thermostat, is designed as depicted in **Fig. 2**a and Fig. S1b and c. The Peltier modules and the thermistor are connected to a temperature thermostat to form a closed-loop temperature controlling system. The measurement of the output voltage is carried out during either heating or cooling the PyEH.

In the experimental test, the temperature fluctuation is a periodic function of time *t*, given by

$$\Delta T = \frac{\Delta T_{\max}}{2}\left[1-\cos\left(\omega t\right)\right], \tag{2}$$

where $\Delta T_{\max}$ is the maximum temperature fluctuation, and ω is the angular frequency. For $\omega = 0.149$ and initial temperature $T\ (t = 0) = 30\ ^{\circ}\mathrm{C}$, three groups of experiments each with the maximum temperature fluctuation $\Delta T_{\max} = 2$, 3 and 4 °C, respectively, are performed as shown in Fig. 2b. The temperature range (30 °C – 34 °C) is small and limited within the operating temperature of the PVDF film (-10 °C – 65 °C, according to the guideline from the manufacturer) to ensure the stability of the pyroelectric properties. For each group of maximum temperature fluctuation, three voltmeters with different inner resistance value R_V = 10 MΩ (Agilent 34450A), 150 GΩ (Agilent B2912A), and 200 TΩ (Keithley 6517B) are used to measure the voltage of the same PyEH, respectively, while their capacitances are all around 360 pF. As shown in Fig. 2c, three different modes of the voltage response are obtained: 1) For R_V = 10 MΩ, the output voltage curves alternate between positive and negative values as a periodic function, which are similar to various results in the literature.[18-34] 2) For R_V = 150 GΩ, the positive voltage curves transit to the periodic function

that is similar as that in case 1) after four cycles. [32] 3) For R_V = 200 TΩ, most portion of the voltage curves becomes positive, which is rarely obtained in the literature. The peak values of the first period are 0.0247 V, 49.9 V, and 56.7 V for the voltmeter with resistances R_V = 10 MΩ, 150 GΩ, and 200 TΩ, respectively, when the temperature fluctuation ΔT_{max} = 4 °C is the same for all cases. The peak value of the voltage output significantly increases with the resistance of the voltmeter, and the difference can be as large as 2296 times. The measured values so depend not only on the pyroelectric device itself, but also the instrument used, which is contrary to the established assumption of set-up independent experimental results. In addition, the increasing of the peak value of the output voltage is mainly caused by the greatly increasing amplitude of the voltage curve when R_V changes from 10 MΩ to 150 GΩ, while the upward shift of the curve rather than the amplitude change dominates the increasing of the peak values when R_V changes from 150 GΩ to 200 TΩ. It is worth pointing out that due to the limitation of the temperature controller used in the experiment, the temperature loads in Fig. 2c are not perfect sinusoidal curves. This leads to the difference in the shape of the curve between the experimental and theoretical voltage with the 10-MΩ-resistance voltmeter, which does not affect our main conclusion.

Furthermore, the temperature change consisting of heating at a constant rate v_T, keeping the temperature unchanged, and cooling to the initial temperature at the same rate was applied on the PyEH. The 10-MΩ-resistance (Keysight 34972, with the capacitance of 360 pF) and the 200-TΩ-resistance voltmeter were used to measure the output voltage, as shown in Fig. S2 and S3. At the end of the heating process, voltages decays to zero as fast as possible in the results of 10-MΩ-resistance voltmeter, while a slower but non-negligible decay can be observed in the results of 200-TΩ-

resistance voltmeter. Another important conclusion is that the peak voltage increases with the increase of v_T rather than ΔT_{max} when the 10-MΩ-resistance was used; on the contrary, the peak voltage depends on ΔT_{max} rather than v_T when measured by a 200-TΩ-inner-resistance voltmeter.

Here, an analytic model is developed to understand the above problem. Only the primary pyroelectric effect needs to be considered,[35] since the PVDF film is mechanical clamped by the temperature controller, i.e. the strain $\varepsilon_{ij} = 0$ ($i, j = 1, 2, 3$), and the temperature change is slow. The linear constitutive model of the PVDF film, i.e. $D_i = k_{ij}E_j + p_i\Delta T$ ($i, j = 1, 2, 3$), gives the relationship among the electric displacement D_i, the electric field E_j and the temperature ΔT, where k_{ij} and p_i are the permittivity and pyroelectric coefficient, respectively. Let the origin of the coordinate system be at the geometric center of the square PVDF film, x_1 and x_2 be in the plane, and the polarization direction x_3 be perpendicular to the surface. The configuration of the system yields that the electric field along x_1 and x_2 are zero, i.e. $E_1 = E_2 = 0$, which, together with $E_3 = V/d$, gives

$$D_3 = \frac{k_{33}V}{d} + p_3\Delta T\,. \tag{3}$$

The output voltages measured with a voltmeter are often recognized as the open-circuit voltage in the literature.[21-26, 30] In those cases, the electric displacement D_3 is zero and the voltage is proportional to the temperature fluctuation, which yield the ideal open-circuit voltage as given in Eq. (1).[9, 35] These results predict that the sign of the output voltage is always same as the temperature fluctuation ΔT. Contrary to this, reported measurements[18-34] and our experimental results (Fig. 2c) show alternating positive and negative values, even for the experiments in which the temperature fluctuation ΔT does not change in sign.

This confliction can be attributed to the underlying hypothesis that the voltmeter has an infinite inner resistance and zero capacitance, while they actually are both with finite values R_V and C_V, respectively, which allow the charge to pass through, stay and change the direction, as shown in **Fig. 3**a. The PyEH can be considered as a capacitor-type charge generator connected in parallel with a resistance with $R_{PyEH} = \rho d/A$, where ρ is the volume resistivity. The currents of the four components in the circuit are related by

$$I_{C\_PyEH} = I_{R\_PyEH} + I_{R\_V} + I_{C\_V}, \tag{4}$$

where $I_{C\_PyEH} = -A\mathrm{d}D_3/(\mathrm{d}t)$ is the current driven by the temperature fluctuation; $I_{C\_V} = C_V\mathrm{d}V/(\mathrm{d}t)$ is the current charging the capacitor of the voltmeter; $I_{R\_V} = V/R_V$ and $I_{R\_PyEH} = V/R_{PyEH}$ are currents passing through the resistances of the voltmeter and the PyEH, respectively. Substitution of the above current into Eq. (4), which, together with Eq. (3), gives

$$\left(C_V + \frac{Ak_{33}}{d}\right)\frac{\mathrm{d}V}{\mathrm{d}t} + V\left(\frac{1}{R_{PyEH}} + \frac{1}{R_V}\right) = -p_3 A\frac{\mathrm{d}\Delta T}{\mathrm{d}t}. \tag{5}$$

With the initial condition $V(t=0) = \Delta T(t=0) = 0$, Eq. (5) yields

$$V = \frac{(-p_3)A}{C_V + \frac{Ak_{33}}{d}}\left[\Delta T - \frac{\frac{1}{R_{PyEH}} + \frac{1}{R_V}}{C_V + \frac{Ak_{33}}{d}} e^{-\frac{\frac{1}{R_{PyEH}} + \frac{1}{R_V}}{C_V + \frac{Ak_{33}}{d}}t} \int_0^t \Delta T e^{\frac{\frac{1}{R_{PyEH}} + \frac{1}{R_V}}{C_V + \frac{Ak_{33}}{d}}t}\,\mathrm{d}t\right]. \tag{6}$$

Fig. 2c shows the curves of the voltage V versus time t obtained from Eq. (6). The theoretical results agree very well with the experimental findings, including both peaks and shapes of the voltage–time curves. The resistance of the voltmeter yields the 'leakage' of the charge for the cases of R_V = 10 MΩ and 150 GΩ, which are smaller than the resistance of the PyEH R_{PyEH} = 1.6 TΩ. For the case of R_V = 200 TΩ, the resistance of the PyEH dominates the slight decay of the voltage-time curves. These

findings confirm that the measured output voltages indeed depend on the resistance of the voltmeter for pyroelectric devices.

In the above experiment and analysis, the capacitance of the voltmeters, C_V = 360 pF, is comparable with the effective capacitance of the PyEH, Ak_{33}/d = 350 pF, of which the influence is nonnegligible. The effects of the capacitance of the voltmeter on the output voltage should also be studied. Experimentally, the capacitance of the voltmeter is changed to C_V = 360 pF, 0.5, 1.1, and 2.2 μF, respectively, by means of an additional capacitance in parallel in the circuit. For R_V = 10 MΩ (Agilent 34450A) and ΔT_{max} = 4 °C, the effect of the capacitance of the voltmeter on the output voltage is shown in Fig. 3b. For R_V = 200 TΩ and ΔT_{max} = 4 °C, the C_V = 360 pF, 1.36, 2.56, and 4.86 nF were used in the experiments, as shown in Fig. S4. The experimental and theoretical results consistently show that the peak value of the output voltage significantly decreases with the increases of the capacitance of the voltmeter. It is found that the measured output voltages also depend on the capacitance of the voltmeter for pyroelectric devices.

Furthermore, it is found that the voltage-time curves still show an overall decay even though the inner resistance of the voltmeter reaches a value as large as R_V = 200 TΩ (Fig. 2c). This finding can be attributed to that the resistance of the PyEH R_{PyEH} = 1.6 TΩ is much smaller than R_V. It yields that the charge 'leaks' via the PyEH itself, that is, the pyroelectric current flows mainly through the resistance of the PyEH rather than the voltmeter. In order to verify this finding, another sample consisting of 16 pieces of the PVDF film (0.8 cm × 0.8 cm × 470 μm) connected in series by 15 μm-thick Al electrodes and copper clad laminates is prepared, as shown in **Fig. 4**a. It is ensured that all the pieces of the PVDF films undergo the same temperature fluctuations during experiments. For the

permittivity $k_{33} = 7\times10^{-11}$ F m^{-1} and the volume resistivity $\rho = 8\times10^{12}$ Ω m, the equivalent capacitance $Ak_{33}/d = 0.60$ pF and the resistance $R_{PyEH} = 940$ TΩ can be obtained according to the equivalent circuit as depicted in Fig. 4b. By the same method of the experimental testing ($R_V = 200$ TΩ and $C_V = 360$ pF) and theoretical analysis ($p_3 = -1.8\times10^{-5}$ C m^{-2} K^{-1}), the voltage-time curves for $\Delta T_{max} = 2$, 3, and 4 °C are obtained in Fig. 4c. The consistent results show that the voltage is always positive and linearly proportional to the temperature without any decay in the investigated range of times, which confirms the validity of the above investigated mechanism.

In principle, the measured results should not depend on the measuring instrument. For the ideal case of $R_V \to \infty$ and $C_V \to 0$, the intrinsic output voltage is obtained or defined, according to Eq. (6), as

$$V_{\text{intrinsic}} = \frac{(-p_3)d}{k_{33}}\left[\Delta T - \frac{d}{Ak_{33}R_{\text{PyEH}}} e^{-\frac{d}{Ak_{33}R_{\text{PyEH}}}t} \int_0^t \Delta T e^{\frac{d}{Ak_{33}R_{\text{PyEH}}}t}\, \mathrm{d}t\right]. \quad (7)$$

When the resistance of the PyEH approaches infinite, i.e. $R_{PyEH} \to \infty$, Eq. (7) reduces to Eq. (1) for the open-circuit voltage used in the literature.[9, 18-34] Since R_{PyEH} is the intrinsic property of the PyEH, the behavior of the decay must appear in the voltage-time curves, no matter how large the resistance of the voltmeter R_V is. The only difference is the rate of decay (fast for Fig. 2c; slow for Fig. 4c). Therefore, the intrinsic output voltage in Eq. (7), instead of the open-circuit voltage, is actually the result that should be obtained to characterize the performance of the PyEH.

The ideal conditions for the voltmeter to get the intrinsic voltage are $R_V >> R_{PyEH}$ (or $R_V \to \infty$) and $C_V << Ak_{33}/d$, which might be impractical for many cases. For instance, all the above experimental tests do not satisfy these conditions, and none of the obtained results is the intrinsic voltage. Fig. 4d shows the comparison of the experimentally obtained results from Fig. 4c and the

intrinsic voltage from Eq. (7). The peaks have a difference as large as 630 times of amplitude, although the shapes of the curves are the same. This huge difference is generated because the capacitance of voltmeter C_V = 360 pF is much larger than that of the PyEH Ak_{33}/d = 0.60 pF. The driven charge is shared, and the voltage is reduced by the capacitance of the voltmeter. Therefore, the present findings suggest that the resistance and the capacitance of the voltmeter should be reported for voltage measurement of the pyroelectric devices, so that researchers can compare the performance of the devices scientifically.

3. Conclusion and outlook

In summary, the output voltage measurement is of fundamental importance to characterize the performance of the advanced PyEH. Experimental investigations in the literature show that the voltage–time curves of pyroelectric devices encompass both positive and negative characteristics, even though the applied temperature fluctuation ΔT is always positive. This phenomenon does not obey the pyroelectric theory for open circuit, which is usually deployed to quantitatively predict the peak voltage in the literature. Here, this problem is addressed by both the theoretical model and experimental measurements. Collective results show that the measured output voltage strongly depends on both the resistance and the capacitance of the voltmeter. The peak of voltage increases with the increase of the resistance and the decrease of the capacitance of the voltmeter, with variations found spanning a factor as large as 2296 times. In many cases, the open-circuit output voltage cannot be directly accessible by experiments, because the resistance of the PyEH may yield local ‘leakage’ of the generated charge. The intrinsic output voltage, instead of the open-circuit output voltage, is actually the result that should be obtained to characterize the performance of the PyEH. As a

significant conclusion, the value of the resistance and of the capacitance of the measurement system should be reported in studies on voltage measurements of pyroelectric devices, so that researchers can compare the performance of the various devices scientifically.

This finding and conclusion can also be extended to other pyroelectric devices and other functional devices, including thermoelectric, piezoelectric and photoelectric energy-harvesting systems. Among them, the piezoelectric energy harvesting system has been discussed preliminarily in our previous works. [36, 37] However, the influence of the capacitance of the voltmeter and the finite resistance of the piezoelectric material has not been considered. We believe that the new findings and conclusions in this work need to be extended to the piezoelectric devices in turn. In addition, the output current under a given load is another key parameter to evaluate the performance of energy harvesting systems. A comprehensive and intensive study was conducted by G. Zhang, Q. Liao and Y. Zhang *et al*. in the field of the piezoelectric energy harvesting. [38] In this excellent work, one important conclusion is that the peak piezoelectric current is sensitive to the load resistance, capacitance, and the strain rate. The maximum peak current (MPC) which is independent of strain rate was proved to exist. A rationally design procedure was proposed to measure the MPC, which gives a new guideline to characterize the performance of the piezoelectric energy harvester. We believe that these findings and conclusions can be extended to the PyEH as well, which need to be investigated further.

4. Experimental Section

Fabrication of the PyEH: Metal coated and polarized PVDF films with thickness of 110 μm and 500 μm were purchased from ZHIMK technology (Shenzhen) CO. LTD. The two kinds of PVDF

film have sandwich structures of Ag/PVDF/Ag (15 μm/80 μm/15 μm) and Al/PVDF/Al (15 μm/470 μm/15 μm), respectively. They were cut by hand into the required size (2 cm × 2 cm for the thinner PVDF film and 0.8 cm × 0.8 cm for the thicker one). Copper clad laminates are used to connect the PVDF films in series and to connect PyEH to the external measuring circuit. Electrical contacts were fixed with conductive silver adhesive and polyimide tape was used to cover the exposed copper to avoid unnecessary circuit connections.

Experimental set up: The PyEH was sandwiched between two Peltier modules, with thermal pads placed between them to ensure the rapid temperature response and uniform temperature distribution. An NTC thermistor was placed next to the PyEH to measure the temperature. On the top and bottom of the device were heatsinks, which were used to not only dissipate heat but also hold the PyEH tightly to ensure the mechanical clamping boundary condition.

Temperature control was achieved by a TCM-M115 thermostat with the precision of 0.001 °C, which was purchased from Chengdu Yexian Tech CO. LTD. Output voltages of the PyEH were measured by voltmeters with inner resistance R_V = 10 MΩ (Agilent 34450A and Keysight 34972), 150 GΩ (Agilent B2912A), and 200 TΩ (Keithley 6517B). The Agilent 34450A was used in the experiments of Fig. 2 and 3, while the Keysight 34972 was used in the experiments of Fig. S2 - S4. Capacitance of the voltmeters was measured by a digital AC bridge @100 Hz. Due to the parasitic capacitance inevitably caused by the test circuit and the copper clad laminates, the measured results were considered to the total capacitance of the voltmeter, which are all around 360 pF.

Acknowledgements

This work was supported by the National Natural Science Foundation of China (grants 11772331 and 11572323), Beijing Municipal Science and Technology Commission (Z191100002019010), Beijing Municipal Natural Science Foundation (No. 2202066), Key Research Program of Frontier Sciences of the Chinese Academy of Sciences (ZDBS-LY-JSC014), Chinese Academy of Sciences via the "Hundred Talent Program", Strategic Priority Research Program of the Chinese Academy of Sciences (No. XDB22040501), Beijing Institute of Space Mechanics & Electricity, and the State Key Laboratory of Structural Analysis for Industrial Equipment, Dalian University of Technology (No. GZ19102).

References

[1] X. Wang, Z. Liu, T. Zhang, Small, 13 (2017) 1602790.

[2] P. Gutruf, J.A. Rogers, Curr. Opin. Neurobiol., 50 (2018) 42-49.

[3] S. Kumar, B.G. Falzon, S.C. Hawkins, Carbon, 149 (2019) 380-389.

[4] Z.L. Wang, Adv. Mater., 24 (2012) 280-285.

[5] H. Ryu, H.J. Yoon, S.W. Kim, Adv. Mater., 31 (2019) 1802898.

[6] Y. Bai, H. Jantunen, J. Juuti, Adv. Mater., 30 (2018) 1707271.

[7] Y. Zhou, C.H. Wang, W. Lu, L. Dai, Adv. Mater., 32 (2020) 1902779.

[8] J. Chmiola, C. Largeot, P.-L. Taberna, P. Simon, Y. Gogotsi, Science, 328 (2010) 480-483.

[9] C.R. Bowen, J. Taylor, E. LeBoulbar, D. Zabek, A. Chauhan, R. Vaish, Energy Environ. Sci., 7 (2014) 3836-3856.

[10] D. Lingam, A.R. Parikh, J. Huang, A. Jain, M. Minary-Jolandan, Int. J. Smart Nano Mat., 4 (2013) 229-245.

[11] H. Ryu, S.W. Kim, Small, (2019) 1903469.

[12] T. Yu, G.Z. Zhang, Y. Yu, Y.K. Zeng, S.L. Jiang, Sens. Actuator A-Phys., 223 (2015) 159-166.

[13] G.Z. Zhang, P. Zhao, X.S. Zhang, K. Han, T.K. Zhao, Y. Zhang, C.K. Jeong, S.L. Jiang, S.L. Zhang, Q. Wang, Energy Environ. Sci., 11 (2018) 2046-2056.

[14] E. Meirzadeh, D.V. Christensen, E. Makagon, H. Cohen, I. Rosenhek-Goldian, E.H. Morales, A. Bhowmik, J.M.G. Lastra, A.M. Rappe, D. Ehre, M. Lahav, N. Pryds, I. Lubomirsky, Adv. Mater., 31 (2019) 1904733.

[15] Q. Leng, L. Chen, H. Guo, J. Liu, G. Liu, C. Hu, Y. Xi, J. Mater. Chem. A, 2 (2014) 11940-11947.

[16] X. Xu, L. Xiao, Y. Jia, Z. Wu, F. Wang, Y. Wang, N.O. Haugen, H. Huang, Energy Environ. Sci., 11 (2018) 2198-2207.

[17] Z. Han, S. Ullah, G. Zheng, H. Yin, J. Zhao, S. Cheng, X. Wang, J. Yang, Ceram. Int., 45 (2019) 24493-24499.

[18] J.H. Lee, H. Ryu, T.Y. Kim, S.S. Kwak, H.J. Yoon, T.H. Kim, W. Seung, S.W. Kim, Adv. Energy Mater., 5 (2015) 1500704.

[19] M. Shen, W. Li, M.Y. Li, H. Liu, J. Xu, S. Qiu, G. Zhang, Z. Lu, H. Li, S. Jiang, J. Eur. Ceram. Soc., 39 (2019) 1810-1818.

[20] C.M. Wu, M.H. Chou, T.F. Chala, Y. Shimamura, R.i. Murakami, Compos. Sci. Technol., 178 (2019) 26-32.

[21] H. Liu, T. Zhao, W. Jiang, R. Jia, D. Niu, G. Qiu, L. Fan, X. Li, W.P. Liu, B. Chen, Y. Shi, L. Yin, B. Lu, Adv. Funct. Mater., 25 (2015) 7071-7079.

[22] Y. Yang, S. Wang, Y. Zhang, Z.L. Wang, Nano Lett., 12 (2012) 6408-6413.

[23] D. Zabek, J. Taylor, C.R. Bowen, IEEE Trans. Ultrason. Ferroelectr. Freq. Control, 63 (2016) 1681-1689.

[24] T. Ding, L. Zhu, X.Q. Wang, K.H. Chan, X. Lu, Y. Cheng, G.W. Ho, Adv. Energy Mater., 8 (2018) 1802397.

[25] A. Sultana, S.K. Ghosh, M.M. Alam, P. Sadhukhan, K. Roy, M. Xie, C.R. Bowen, S. Sarkar, S. Das, T.R. Middya, D. Mandal, ACS Appl. Mater. Interfaces, 11 (2019) 27279-27287.

[26] A. Kumar, S. Kumar, S. Patel, M. Sharma, P. Azad, R. Vaish, R. Kumar, K.S. Srikanth, J. Intell. Mater. Syst. Struct., 30 (2019) 869-877.

[27] K. Zhang, Z.L. Wang, Y. Yang, ACS Nano, 10 (2016) 10331-10338.

[28] J.H. Lee, K.Y. Lee, M.K. Gupta, T.Y. Kim, D.Y. Lee, J. Oh, C. Ryu, W.J. Yoo, C.Y. Kang, S.J. Yoon, J.B. Yoo, S.W. Kim, Adv. Mater., 26 (2014) 765-769.

[29] Y. Yang, J.H. Jung, B.K. Yun, F. Zhang, K.C. Pradel, W. Guo, Z.L. Wang, Adv. Mater., 24 (2012) 5357-5362.

[30] X.-Q. Wang, C.F. Tan, K.H. Chan, K. Xu, M. Hong, S.-W. Kim, G.W. Ho, ACS Nano, 11 (2017) 10568-10574.

[31] D. Zabek, J. Taylor, E.L. Boulbar, C.R. Bowen, Adv. Energy Mater., 5 (2015) 1401891.

[32] T. Zhao, W. Jiang, H. Liu, D. Niu, X. Li, W. Liu, X. Li, B. Chen, Y. Shi, L. Yin, B. Lu, Nanoscale, 8 (2016) 8111-8117.

[33] K. Song, R. Zhao, Z.L. Wang, Y. Yang, Adv. Mater., 31 (2019) 1902831.

[34] X. Chen, J. Shao, X. Li, H. Tian, IEEE Trans. Nanotechnol., 15 (2016) 295-302.

[35] S. Jachalke, E. Mehner, H. Stöcker, J. Hanzig, M. Sonntag, T. Weigel, T. Leisegang, D.C. Meyer, Appl. Phys. Rev., 4 (2017) 021303.

[36] Y. Su, C. Dagdeviren, R. Li, Adv. Funct. Mater., 25 (2015) 5320-5325.

[37] Y.W. Su, S. Li, Y. Huan, R. Li, Z.H. Zhang, P. Joe, C. Dagdeviren, Extreme Mech Lett, 15 (2017) 10-16.

[38] G.J. Zhang, Q.L. Liao, M.Y. Ma, Z. Zhang, H.N. Si, S. Liu, X. Zheng, Y. Ding, Y. Zhang, Nano Energy, 30 (2016) 180-186.

Figures and figure captions

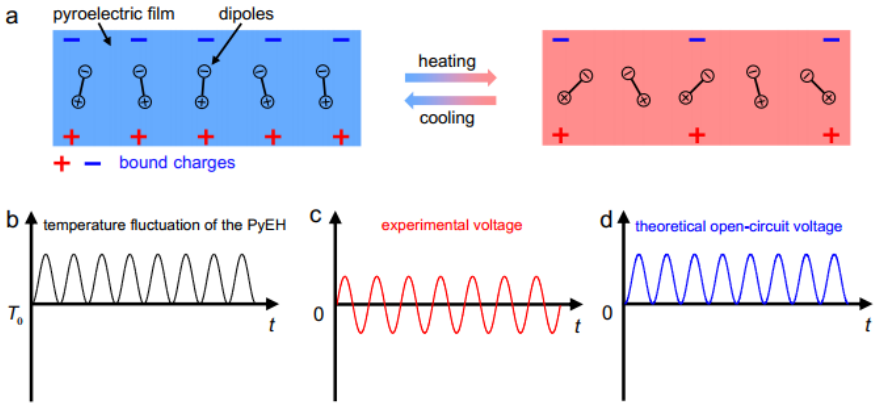

Fig. 1. The confliction between the experimental and theoretical voltage-time curves. (a) Schematic illustration of the basic mechanism of operation of pyroelectric materials. Schematic illustrations of the curves of (b) the temperature fluctuation applied to the PyEH, output voltage versus time from (c) experiments and (d) the pyroelectric theory for the open circuit.

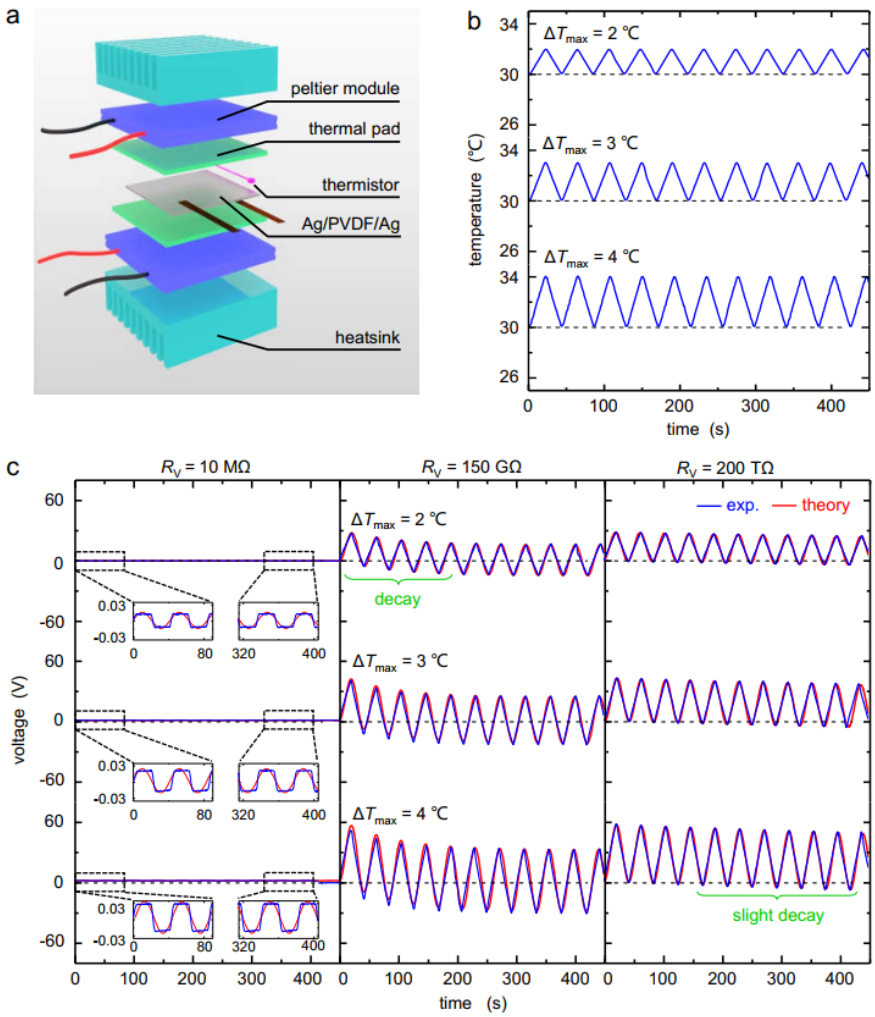

Fig. 2. Experimental results and theoretical prediction of the output voltage of the PyEH. (a) Schematic illustration of the temperature controller for the performance characterization of the PyEH. (b) Temperature fluctuation applied to the PyEH. (c) Voltage curves of the same PyEH measured by three voltmeters with inner resistances of 10 MΩ (left), 150 GΩ (middle), and 200 TΩ (right), respectively.

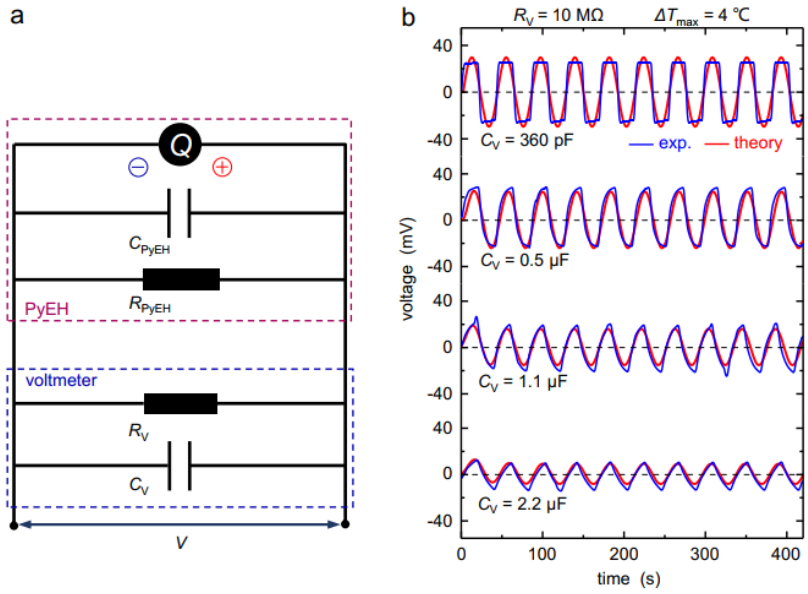

Fig. 3. **The investigation of effects of the capacitance on the output voltage of the PyEH.** (a) Schematic illustration of the measurement circuit considering both of the finite resistance and capacitance of the voltmeter and the PyEH. (b). Effects of the capacitance of the voltmeter on the output voltage.

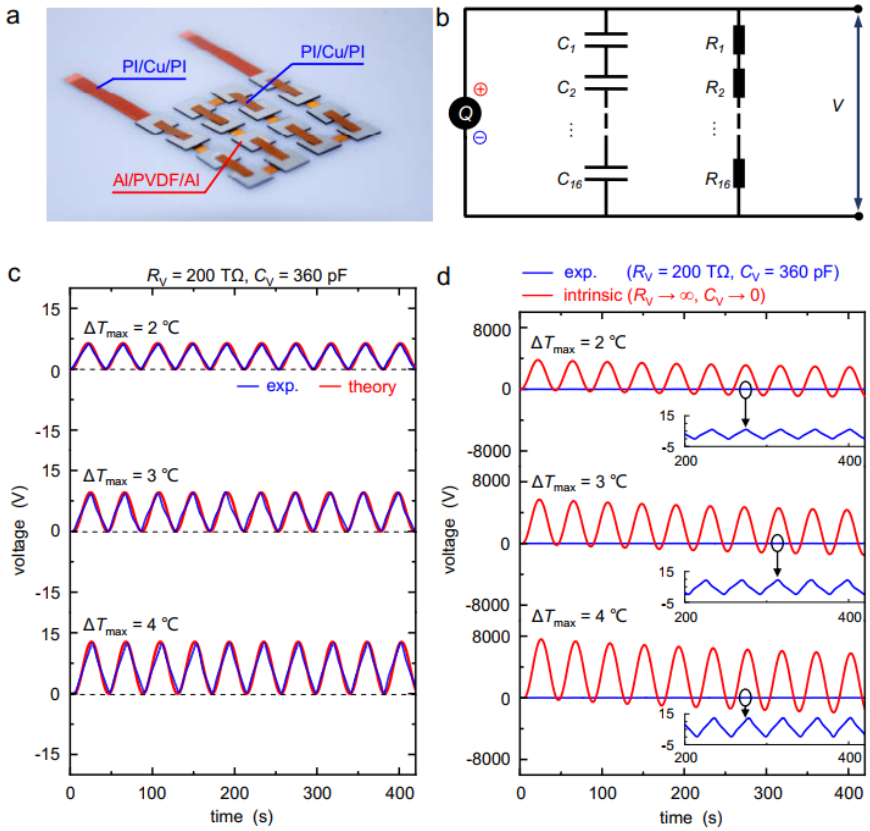

Fig. 4. **The investigation of the comparison of measured output voltage and the intrinsic voltage.** (a) Photograph of the PyEH that consisting of 16 pieces of the PVDF film. (b) Equivalent circuit of the PyEH in (a). (c) Voltage curves of the PyEH in (a) measured by the voltmeter with inner resistance of 200 TΩ. (d). Comparison between the experimental voltage in (c) and the intrinsic voltage of the PyEH in (a).

Published in Nano Energy, doi: 10.1016/j.nanoen.2021.106045 (2021).

Supplementary Information

On the Evaluation of Output Voltages for Quantifying the Performance of Pyroelectric Energy Harvesters

Qinlan Li, [a,b] Shuang Li, [a,b] Dario Pisignano,[c] Luana Persano, [d] Ya Yang, [e] Yewang Su [a,b,f*]

[a] *State Key Laboratory of Nonlinear Mechanics, Institute of Mechanics, Chinese Academy of Sciences, Beijing 100190, China*

[b] *School of Engineering Science, University of Chinese Academy of Sciences, Beijing 100049, China*

[c] *Dipartimento di Fisica, Università di Pisa, Largo B. Pontecorvo 3, I-56127 Pisa, Italy*

[d] *NEST, Istituto Nanoscienze-CNR, Piazza S. Silvestro 12, I-56127 Pisa, Italy*

[e] *CAS Center for Excellence in Nanoscience, Beijing Key Laboratory of Micro-nano Energy and Sensor, Beijing Institute of Nanoenergy and Nanosystems, Chinese Academy of Sciences, Beijing, 100083, China*

[f] *State Key Laboratory of Structural Analysis for Industrial Equipment, Department of Engineering Mechanics, Dalian University of Technology, Dalian 116024, China*

[*] To whom all correspondence should be addressed: yewangsu@imech.ac.cn

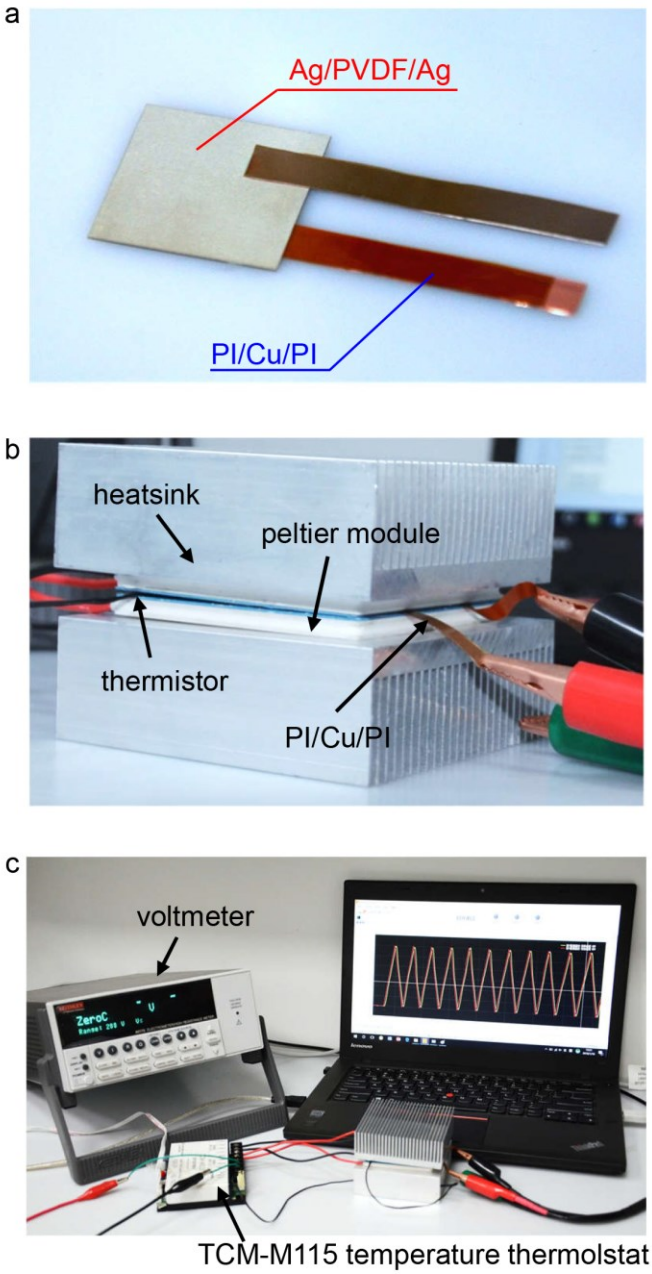

Fig. S1. Photograph of the experimental setup. (a) Photograph of the prepared PyEH. (b) Photograph of the temperature controller for the performance characterization of the PyEH. (c) Photograph of the entire experimental system.

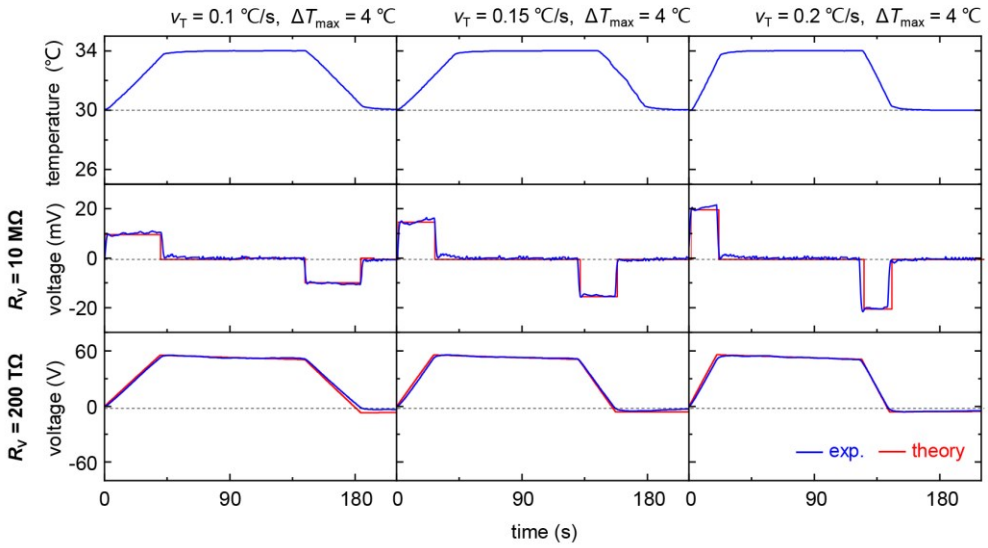

Fig. S2. Measured output voltages when heating and cooling the PyEH at a constant rate v_T. The amplitude was kept at ΔT_{max} = 4 °C and the rate of temperature v_T = 0.1, 0.15, and 0.2 °C/s, respectively. The 10-MΩ-resistance (Keysight 34972) and the 200-TΩ-resistance voltmeter were used.

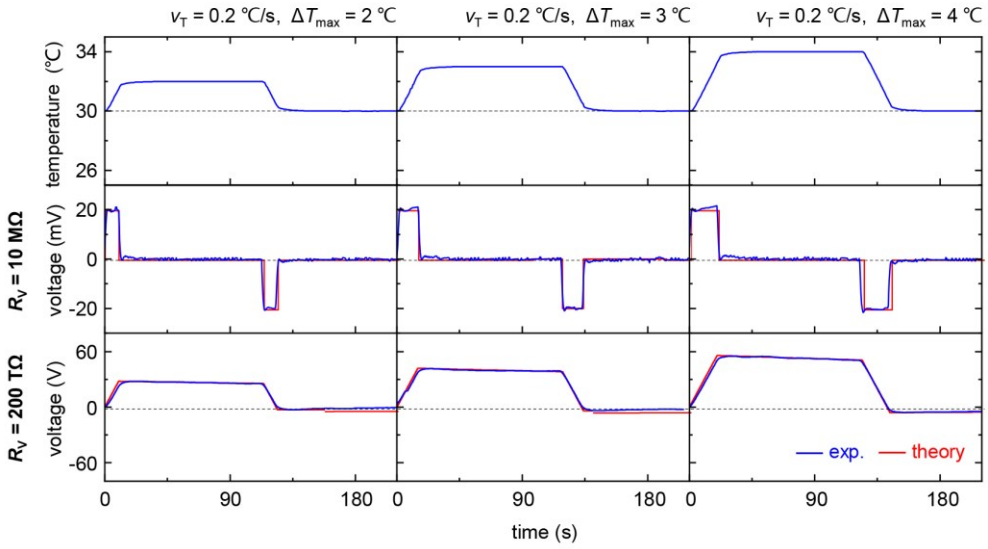

Fig. S3. Measured output voltages when heating and cooling the PyEH at a constant rate v_T. The rate of temperature was kept at v_T = 0.2 °C/s and the amplitude ΔT_{max} = 2, 3, and 4 °C. The 10-MΩ-resistance (Keysight 34972) and the 200-TΩ-resistance voltmeter were used.

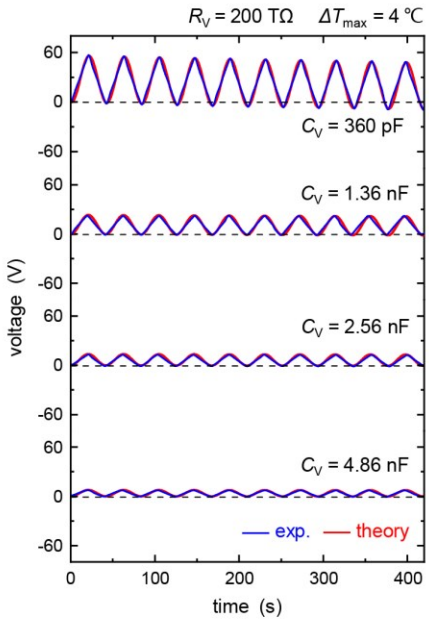

Fig. S4. The investigation of the effect of the capacitance on the output voltage of the PyEH. C_V = 360 pF, 1.36 nF, 2.56 nF, and 4.86 nF, respectively. The 200-TΩ-resistance voltmeter was used.